

## Supporting information

### **Ultrathin in situ silicification layer developed by electrostatic attraction forced strategy for ultrahigh-performance oil-water emulsions separation**

Lei Zhang, Yuqing Lin\*, Haochen Wu, Liang Cheng, Yuchen Sun, Tomoki Yasui,  
Zhe Yang, Shengyao Wang, Tomohisa Yoshioka, Hideto Matsuyama\*

*Research Center for Membrane and Film Technology, Department of Chemical Science and Engineering, Kobe University, Kobe 657-8501, Japan*

\* Corresponding authors

*E-mail:* [yqlin@people.kobe-u.ac.jp](mailto:yqlin@people.kobe-u.ac.jp) (Yuqing Lin)

[matuyama@kobe-u.ac.jp](mailto:matuyama@kobe-u.ac.jp) (H. Matsuyama)

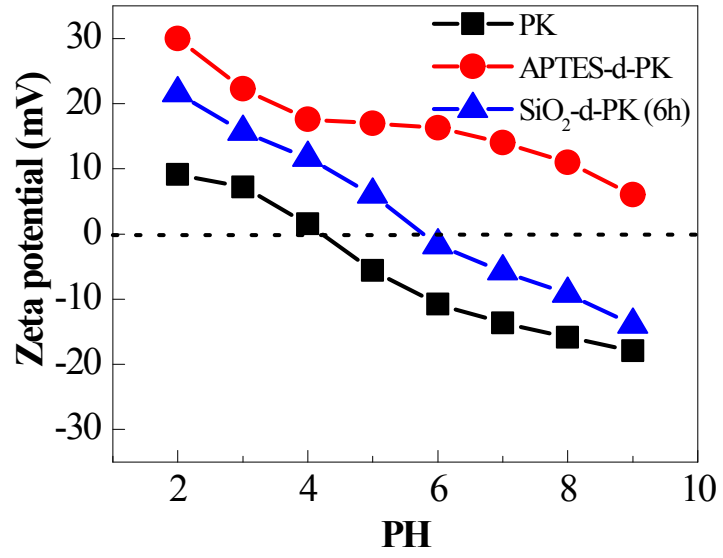


**Fig. S1.** The surface zeta potential of nascent PK substrate, APTES-d-PK membrane, and SiO<sub>2</sub>-d-PK membrane at the PH values of 2-9.

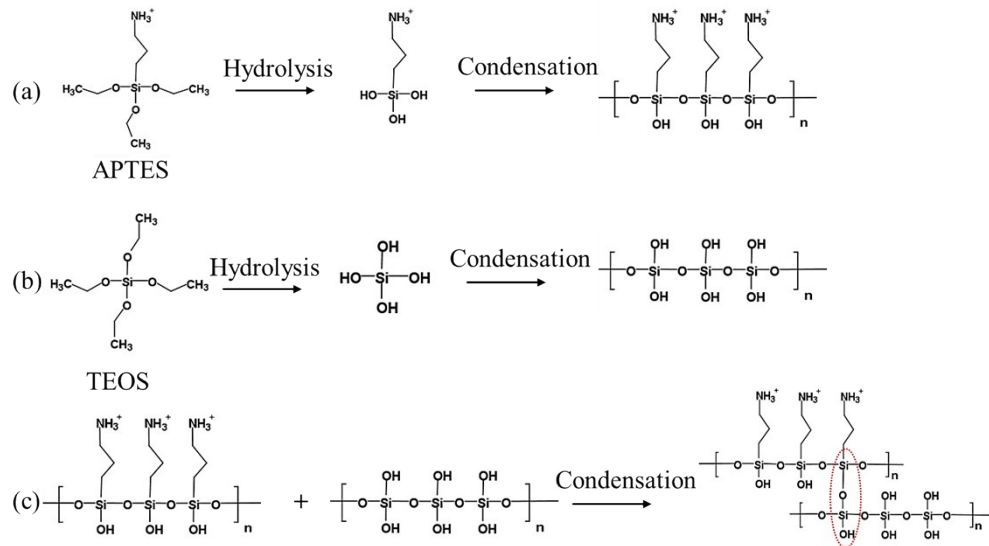


**Fig. S2.** The mechanism of electrostatic attraction forced in-situ surface silicification for the preparation of SiO<sub>2</sub>-d-PK membrane: (a) the hydrolysis and condensation process of APTES monomer; (b) the hydrolysis and condensation process of TEOS monomer; (c) the condensation process between the surface silicification layer with APTES layer.

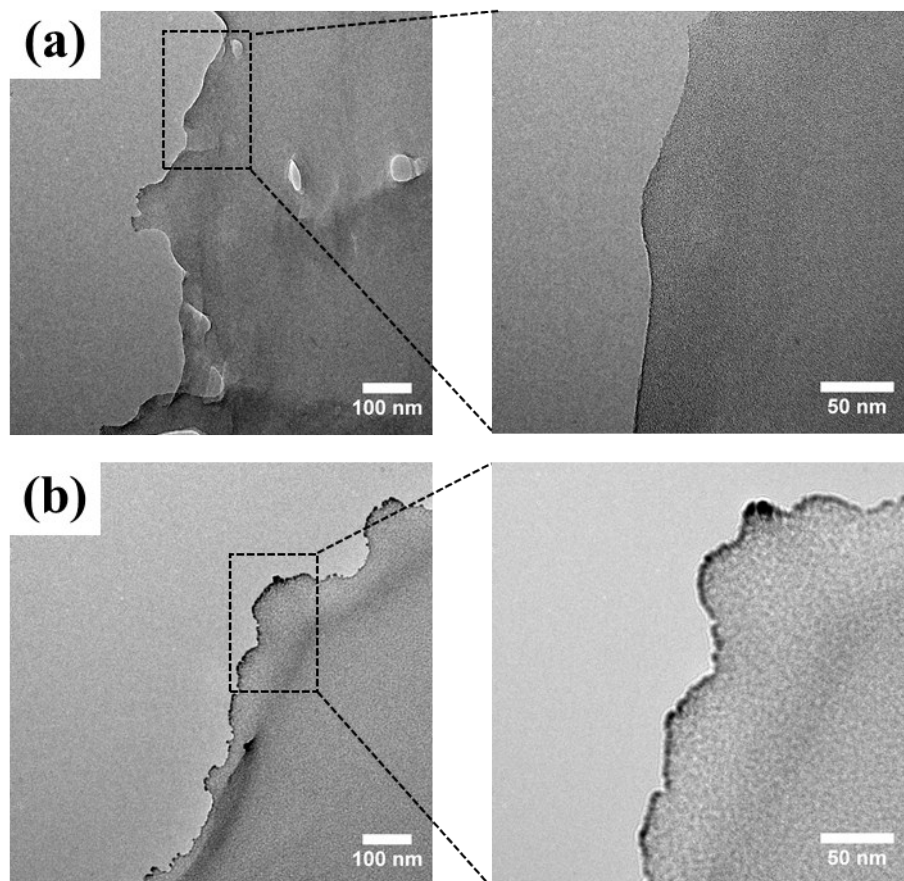


**Fig. S3.** TEM cross-sectional images of (a) PK and (b) SiO<sub>2</sub>-d-PK membranes.

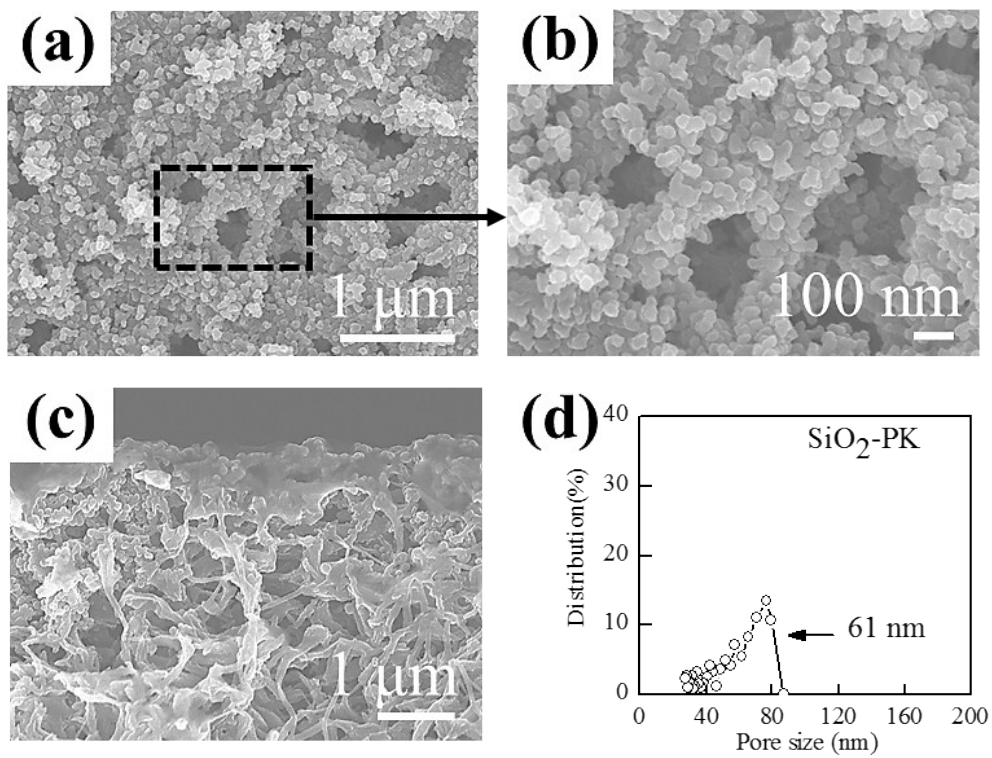


**Fig. S4.** Morphologies and pore size of the SiO<sub>2</sub>-PK membrane without APTES pretreatment:(a) surface morphology; (b) enlarged surface morphology; (c) cross-section morphology; and (d) pore size distribution.

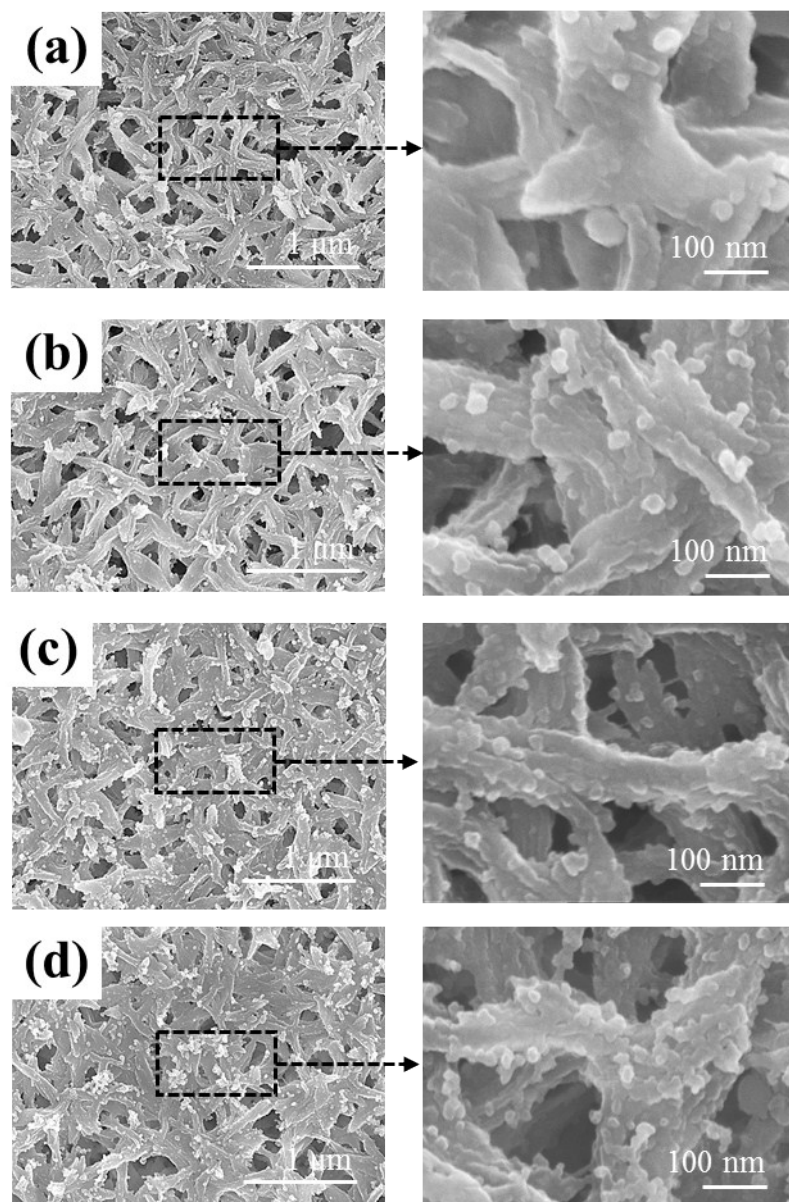


**Fig. S5.** The surface morphologies of SiO<sub>2</sub>-d-PK membranes over the prolonged silicification process: (a) 1h; (b) 3h; (c) 6h; (d) 9h.

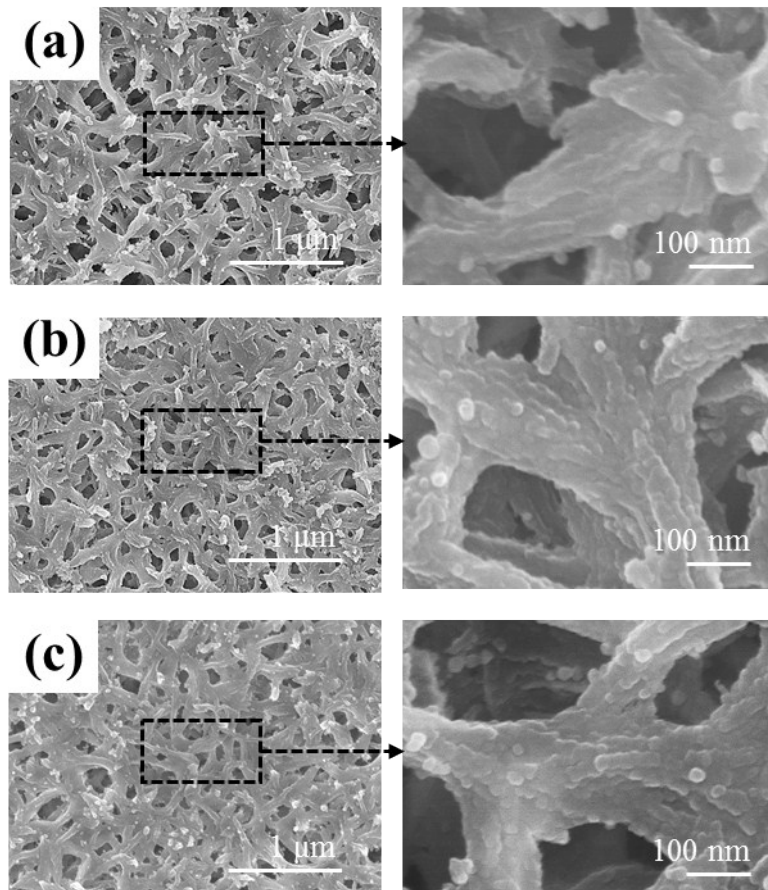


**Fig. S6.** The surface morphologies of SiO<sub>2</sub>-d-PK membranes with different TEOS concentrations under the same surface silicification period of 6 h: (a) 3 ml, (b) 5ml, and (c) 7 ml in 100 ml ethanol solutions.

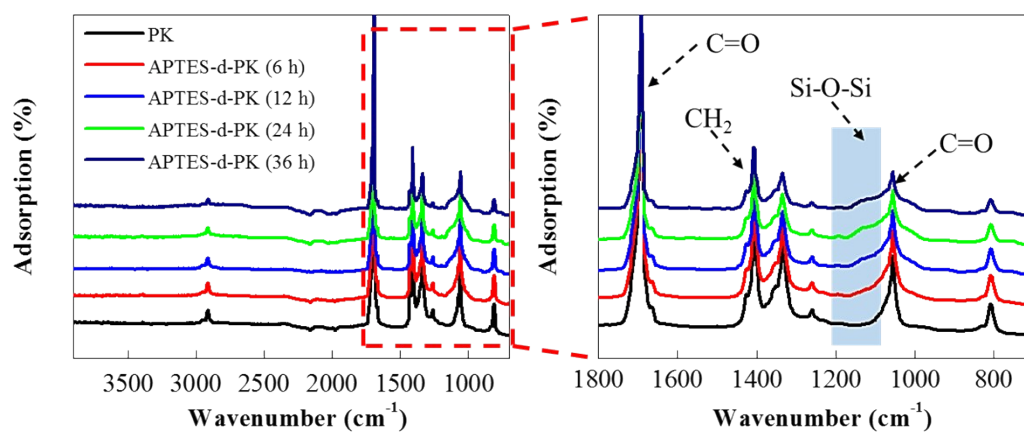


**Fig. S7.** FTIR characterization results of the PK and APTES-d-PK membranes with different deposition time.



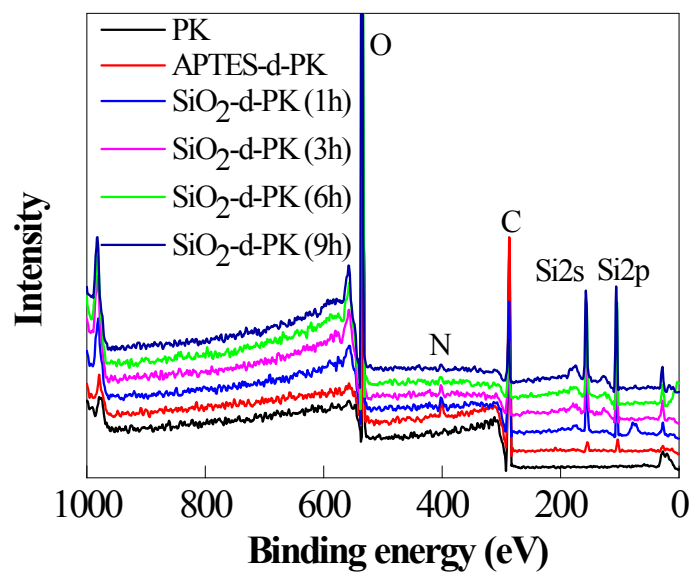


**Fig. S8.** XPS characterization results of PK, APTES-d-PK, and SiO<sub>2</sub>-d-PK membranes.

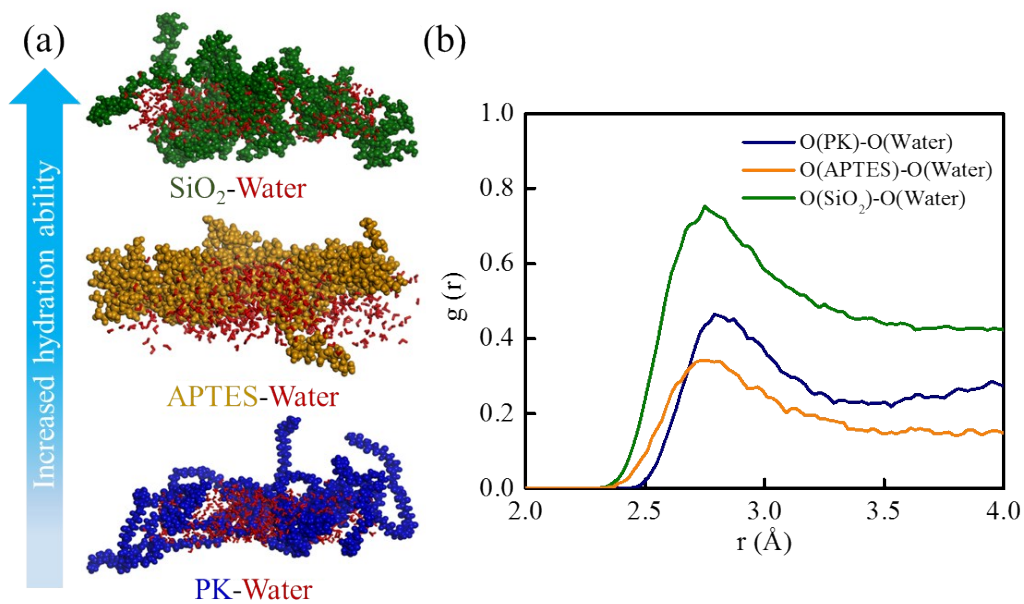


**Fig. S9.** MD simulation results of (a) models between water molecules and PK, APTES, and SiO<sub>2</sub> within 3.5 Å, where the molecular chains are colored as follows: PK: blue; APTES: yellow; SiO<sub>2</sub>: green; water: red; (b) RDF analysis between the oxygen atom of water and the oxygen atoms of PK, APTES, and SiO<sub>2</sub>.

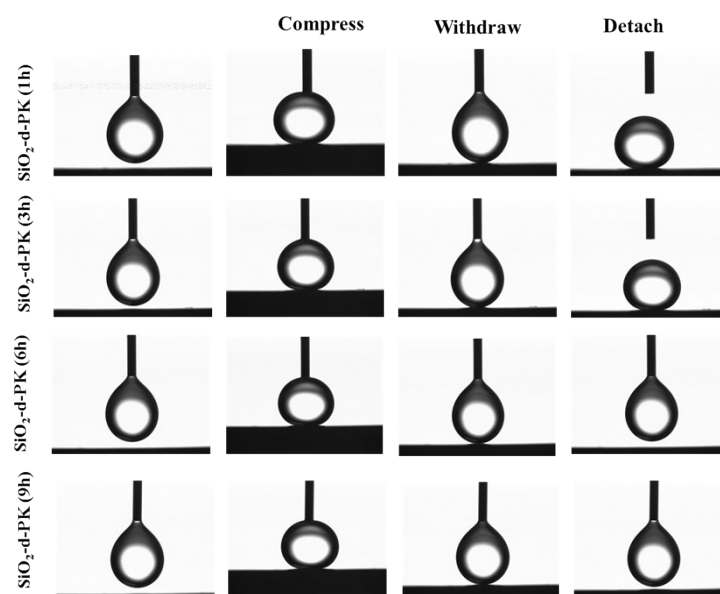


**Fig. S10.** Underwater dynamic oil-adhesion tests on the SiO<sub>2</sub>-d-PK membranes surface prepared under different silicification periods, and the chloroform was used as the probe oil in this test.

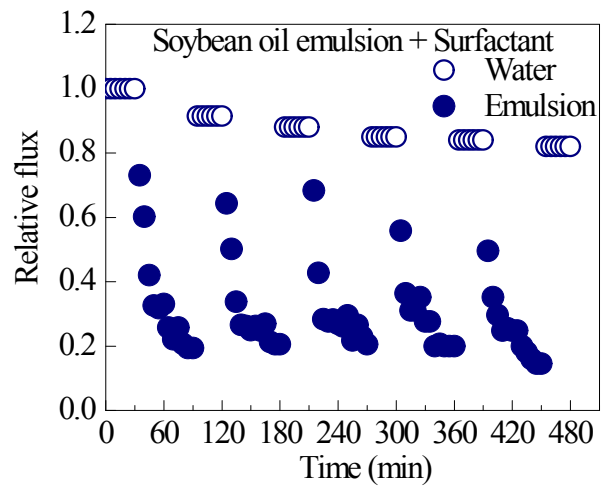


**Fig. S11.** Antifouling property of SiO<sub>2</sub>-d-PVDF membrane for soybean oil-in-water emulsion.

**Table S1.** The surface porosities of the as-prepared membranes

membranes	PK	APTES-d-PK	SiO <sub>2</sub> -d-PK
Surface porosity (%)	44.3 ±4.8	43.4 ±0.8	41.0 ±4.2